Lifetimes and transition dipole moment functions of NaK low lying singlet states: Empirical and *ab initio* approach

M. Tamanis, M. Auzinsh, I. Klincare, O. Nikolayeva, and R. Ferber
Department of Physics, University of Latvia, Riga LV-1586, Latvia

A. Zaitsevskii, E. A. Pazyuk, and A. V. Stolyarov
Department of Chemistry, Moscow M. Lomonosov State University, Moscow 119899, Russia

(Received 22 January 1998; accepted 16 July 1998)

The paper presents experimental $D\,^1\Pi$ state lifetime $\tau_{v'J'}$ data and develops empirical and *ab initio* approaches concerning $D\,^1\Pi$ and $B\,^1\Pi$ lifetimes, as well as $D\,^1\Pi-X\,^1\Sigma^+$, $B\,^1\Pi-X\,^1\Sigma^+$ and $D\,^1\Pi-A\,^1\Sigma^+$ transition dipole moment functions $\mu(R)$ of the NaK molecule. Experimental $D\,^1\Pi(v',J')$ state $\tau_{v'J'}$ values for v' varying from 1 to 22 have been obtained from experimentally measured electric radio frequency-optical double resonance (rf-ODR) signal contours. The rf-ODR signals have been produced by $D\,^1\Pi\leftarrow X\,^1\Sigma^+$ laser induced optical transition and rf field (1–900 MHz) induced $e-f$ transition within the $D\,^1\Pi(v',J')$ level. The possibility to determine empirical absolute $\mu(R)$ function in a wide R range from experimental $\tau_{v'J'}$ dependence on v' and J' has been demonstrated; such an approach has been applied to obtain $\mu(R)$ for the $B\,^1\Pi-X\,^1\Sigma^+$ transition on which relative intensity data are absent. The empirical $D\,^1\Pi-X\,^1\Sigma^+\,\mu(R)$ function has been considerably improved by simultaneous fitting of relative intensity and lifetime data implicitly accounting for the J' dependence of measured lifetime values. The finite-field technique combined with the many-body multipartitioning perturbation theory was used for *ab initio* all-electron transition moment calculations. This approach appeared to be adequate to compute reliable $\mu(R)$ functions due to a proper description of core-valence correlations. As a result, excellent agreement between *ab initio* and empirical $B\,^1\Pi-X\,^1\Sigma^+$ and $D\,^1\Pi-X\,^1\Sigma^+$ transition dipole moment functions has been achieved. © *1998 American Institute of Physics.* [S0021-9606(98)02139-4]

I. INTRODUCTION

It is well known that for such test diatomics as alkali dimers the calculated potential energies agree well enough with the experimental ones (see Ref. 1, and references therein). However, *ab initio* calculations are still less effective in reproducing intensities in molecular spectra arising from excited electronic states. At the same time, such radiative quantities as transition dipole moments $\mu(R)$, the corresponding lifetimes τ and intensity data represent, along with permanent electric dipole moments, a different and, in many cases, an extremely useful test of the validity of calculation methods and of the accuracy of molecular constant sets. This situation reflects the fact that one may expect considerable electron charge redistribution within particular molecular configurations without any substantial impact on the energy of the system.[2] First results obtained in the pioneering papers on homonuclear alkali dimer Na_2 appeared to be quite promising since a very good agreement between empirical[3,4] and calculated[5] $\mu(R)$ has been achieved. It was, however, not the case with the transition dipole moment function $\mu(R)$ for a heteronuclear diatomic molecule NaK. Indeed, a considerable (though not large) discrepancy comes to light if one compares the absolute values of empirical transition dipole moments reported for $D\,^1\Pi-X\,^1\Sigma^+$ transition in the NaK molecule by Pfaff, Stock and Zevgolis (PSZ) in Ref. 6, as well as by Katô and Noda (KN) in Ref. 7, with *ab initio* pseudopotential calculations of the same quantities performed by Ratcliff, Konowalow and Stevens (RKS).[2] Experimental lifetimes of a lower lying NaK $B\,^1\Pi$ state presented by Derouard, Debontride, Nguyen and Sadeghi (DDNS) in Ref. 8 are also significantly different from their theoretical counterparts calculated by exploiting the *ab initio* $B\,^1\Pi-X\,^1\Sigma^+$ transition dipole moment $\mu(R)$ given by RKS. At the same time, the $\mu(R)$ behavior for low lying singlet states of NaK is of general interest because of the much more pronounced R dependence due to the partially ionic character of charge distribution.

It was not easy to judge whether the measured empirical (PSZ, KN, DDNS) or the calculated (RKS) μ and τ values are responsible for such a discrepancy. This circumstance stimulated us to undertake in the present work an attempt to obtain more accurate empirical $\mu(R)$ data, as well as to carry out *ab initio* all-electron calculations using many-body multipartitioning perturbation theory (MPPT),[9] which seems to be more adequate for the description of core-valence correlations than previously used pseudopotential schemes.[2] To obtain more reliable absolute values of the empirical $\mu_{D\text{-}X}(R)$ function for $D\,^1\Pi-X\,^1\Sigma^+$ transition, we have performed lifetime $\tau_{v'J'}$ measurements in a wide range of NaK $D\,^1\Pi$ state vibrational levels v' varying from 1 to 22. These data, along with somewhat corrected $D\,^1\Pi-X\,^1\Sigma^+$ transition relative intensities taken from Ref. 6, have been processed simultaneously in order to gain the empirical $\mu_{D\text{-}X}(R)$ function. An improved method to invert the experimental lifetimes into the $\mu(R)$ function has been applied in order to get the empirical $B\,^1\Pi-X\,^1\Sigma^+$ transition dipole moment. In ad-

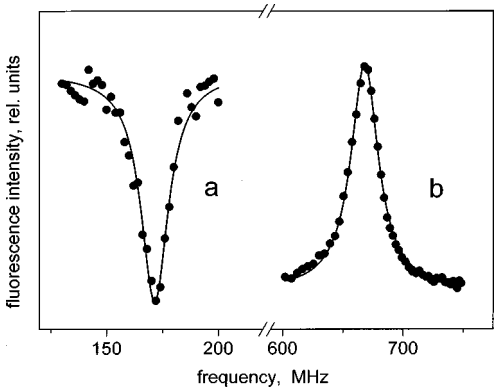

FIG. 1. Experimental NaK $D\,^1\Pi$ state rf-ODR signal contours. (a) $v'=4$, $J'=19$, allowed Q-line, fitting parameters $f_0=171.4$ MHz, $\Delta_{1/2}=14.95$ MHz; (b) $v'=11$, $J'=46$, forbidden Q-line, fitting parameters $f_0=673.7$ MHz, $\Delta_{1/2}=26.48$ MHz. The solid line is a Lorentzian fit, see Eq. (1).

dition, we have undertaken a detailed theoretical study of the transition moment functions at the *ab initio* all-electrons level with accurate treatment of core-valence electron effects.

II. EXPERIMENTAL RESULTS

The most straightforward and well-developed method to measure excited state lifetimes is, of course, to record directly the fluorescence decay kinetics after pulsed laser excitation. It is however also possible, after careful examination of distorting factors, to gain $^1\Pi$ state lifetime data from the electric radio frequency—optical double resonance (rf-ODR) signal contours. The idea of such a method is very simple and goes back to Refs. 10–12. Since each rotational level J'' in the ground $X\,^1\Sigma^+$ state has a definite parity, due to parity selection rule the laser induced transition $D\,^1\Pi(v',J') \leftarrow X\,^1\Sigma^+(v'',J'')$ excites only one (e or f) component of the $^1\Pi$ state Λ doublet. This is why only the (P,R)-doublet lines are emitted at P- or R- type excitation, while, on the contrary, only the Q-singlet lines can be found in the laser induced fluorescence (LIF) spectrum after Q-type excitation. If the external ac electric field frequency is swept in the vicinity of Λ-splitting energy Δ_{ef}, due to electric dipole $e \leftrightarrow f$ transitions one can observe either the resonant appearance of a ''forbidden'' line in the LIF spectrum, or the resonant diminution of ''allowed'' line intensity, thus giving rise to the respective rf-ODR signals, see Fig. 1, centered at the resonance frequency $f_0=\Delta_{ef}/h$.

To obtain NaK $D\,^1\Pi$ state $\tau_{v',J'}$ values, we have exploited the same rf-ODR setup used previously[13,14] for the purpose of Λ-splitting energy determination. Briefly, Ar^+-laser lines (Table I) have been used to excite a number of $D\,^1\Pi(v',J')$ levels of NaK molecules formed in thermal cells at temperatures $T=525-575$ K. The identification of $D\,^1\Pi\,(v',J')$ states in $D\,^1\Pi(v',J') \rightarrow X\,^1\Sigma(v'',J'')$ LIF progression has been based upon the data reported in Ref. 15. rf electric field voltage (usually up to 5 V) was applied to round polished Stark electrodes placed inside the cell with the spacing ~1 mm and swept over the 5–900 MHz range. A monochromator with spectral resolution ~0.03 nm was used to single out the wavelength corresponding to either ''forbidden'' or ''allowed'' line position in LIF spectra. The rf voltage supply scheme was carefully adjusted to avoid parasitic noise and to achieve constant rf electric field amplitude over the frequency sweeping region across the resonance position.

TABLE I. Excitation laser wavelength (λ_{exc}), NaK $D\,^1\Pi$ state v',J' values, rf-ODR resonance FWHM's ($\Delta_{1/2}$) and lifetimes ($\tau_{v'J'}$) obtained in the present work from rf-ODR experiments.

λ_{exc}, (nm)	v'	J'	$\Delta_{1/2}$ (MHz)	τ (ns)
496.5	1	27	14.7±1.1	22.4±1.7
514.4	1	67	···	18.6±0.3[b]
501.7	3	23	17.7±2.9	18.5±3.0
496.5	3	43	17.1±1.4	19.2±1.5
496.5	4	19	14.0±0.4	23.6±0.7
496.5	7	8	16.8±2.7	19.5±3.0[a]
488.0	7	20	16.5±1.3	19.9±1.5[a]
488.0	7	23	16.5±0.9	19.9±0.1
488.0	7	23	···	20.0±0.3[b]
488.0	10	102	···	17.9±0.3[b]
496.5	11	46	24.3±1.1	13.4±0.6[c]
476.5	12	7	25.5±2.0	12.7±1.0[c]
476.5	14	19	17.7±2.0	18.5±2.0
476.5	17	94	···	16.1±0.3[b]
488.0	22	35	20.0±1.0	16.3±0.8

[a]$^{23}Na^{41}K$ isotope.
[b]Reported by Pfaff, Stock, and Zevgolis (PSZ) (Ref. 6).
[c]Levels perturbed by the $d\,^3\Pi$ state.

The rf-ODR signal shape $I(f)$ has been analyzed by Field and Bergeman.[11] In the most simple case of a weak rf field one would arrive at the Lorentz shape contour

$$I(f)=\frac{I_0}{(\Gamma/2\pi)^2+(f-f_0)^2}, \tag{1}$$

where the full width at half maximum (FWHM) of the rf resonance is Γ/π, thus accounting for two natural widths originating from the two Λ components contribution of $\Gamma/2\pi$ each. In Eq. (1) we neglect power broadening due to ac Stark effect. The estimations based on the approach given in Ref. 13 show that a small enough rf voltage is yet able to cause electric dipole transitions between the Λ-doublet components. Both evaluations and test measurements carried out with different rf field amplitudes allowed us to assume that one can neglect the power broadening effects in the particular experimental conditions. In particular, special experiments which included the diminishing of rf field amplitude from 5 to 1 V did not reveal any changes in signal width, thus confirming for us that one can neglect the power broadening effects.

A typical experimentally obtained fixed optical frequency, a rf swept rf-ODR signal recorded at the ''allowed'' Q-line originating from the $D\,^1\Pi$ state level $v'(J')=4(19)$ is presented in Fig. 1(a), while the analogous signal for the ''forbidden'' line originating from 11(46) is presented in Fig. 1(b). Experimental rf-ODR signals have been processed by Lorentz contour, Eq. (1), thus yielding the FWHM values $\Delta_{1/2}$. The FWHM values averaged over a number of measurements in different fluorescent cells are given in Table I. The errors in Table I reflect the discrepancy of the results obtained in different experiments.

As it has been shown in our treatment of the hyperfine (HF) interaction performed in Ref. 14, one can expect some small HF broadening effect upon the resonance signal. Owing to the $\Delta F=0$ selection rule, the HF broadening of the rf signals can be caused only by the difference in the HFS splitting of e and f components. The main cause of such effect for nonperturbed $D\,^1\Pi$ state levels is due to the presence of nonzero off-diagonal (transversal) matrix elements of the electric quadrupole HF interaction operator. Preliminary estimations[14] of HF structure constants performed by an internally contracted configuration-interaction method have shown that the HF broadening effect on the rf-ODR signals is rather small, being of the order of $\sim$0.5 MHz. This broadening effect has been taken into account by a subsequent correction of experimentally measured $\Delta_{1/2}$ values. The corrected $\Delta_{1/2}$ values have been used to pass to the lifetimes $\tau_{v'J'}=\Gamma^{-1}$. The $\tau_{v'J'}$ values thus obtained are listed in Table I, which also contains the lifetimes presented by PSZ[6] for four $D\,^1\Pi(v',J')$ levels of the NaK molecule. Surprisingly good agreement of the $v'(J')=7(23)$ lifetime $\tau_{v'J'}=19.9\pm1.1$ ns obtained by us from the rf-ODR signal FWHM with $\tau_{v'J'}=20.0\pm0.3$ ns obtained by PSZ from fluorescence decay kinetics, see Table I, encouraged us to believe that our experimental rf-ODR contours can be used to get reliable lifetime values. It has, however, to be noted that, as pointed out in Ref. 14, although the isolated NaK $D\,^1\Pi$ state levels should exhibit only negligible HF broadening of rf-ODR signals, the latter may not be true for the levels which are perturbed by the adjacent $d\,^3\Pi$ state. For such levels one may expect an additional HF broadening caused by the HF nuclear spin–electron spin dipole interaction which is different for e and f components. Another cause for rf signal broadening by the $d\,^3\Pi-D\,^1\Pi$ mixing may appear in cases when the adiabatic lifetimes of triplet levels are shorter than the ones of the $D\,^1\Pi$ state. To exclude the influence of singlet–triplet interaction effects on empirical determination of $D-X$ transition moment functions, the experimental data for the perturbed $v(J)$ levels 11(46) and 12(7) were excluded from the data processing routine.

III. EMPIRICAL DETERMINATION OF TRANSITION DIPOLE MOMENT FUNCTIONS

A. Method

It is well known that both radiative lifetimes ($\tau_{iv'J'}$) and relative $v'J'\rightarrow v''J''$ fluorescence intensities ($I_{ij}^{v'J'v''J''}$) can be used for the empirical determination of R dependence of the transition moment $\mu_{ij}(R)$:[16]

$$\tau_{iv'J'}^{-1}=\frac{8\pi^2}{3\hbar\epsilon_0}\sum_{jv''J''}(\nu_{ij}^{v'J'v''J''})^3(\mu_{ij}^{v'J'v''J''})^2\frac{S_{J'J''}}{2J'+1}, \tag{2}$$

$$\frac{I_{ij}^{v'J'v''J''}}{I_{ij}^{v'J'v''_{\max}J''}}=\left(\frac{\nu_{ij}^{v'J'v''J''}}{\nu_{ij}^{v'J'v''_{\max}J''}}\right)^n\left(\frac{\mu_{ij}^{v'J'v''J''}}{\mu_{ij}^{v'J'v''_{\max}J''}}\right)^2, \tag{3}$$

where $8\pi^2/3\hbar\epsilon_0=2.026\times10^{-6}$, ϵ_0 is the permittivity of vacuum, τ is in s, μ_{ij} in a.u., and ν_{ij} is the rovibronic transition wave number in reciprocal centimeters. Here $n=3$ under photon counting and $n=4$ under intensity measurements in energy units, $S_{J'J''}$ is the Hönl–London factor, $v''_{\max}$ corresponds to the band with maximal intensity within a given progression, and $\mu_{ij}^{v'J'v''J''}$ is treated as[17]

$$\begin{aligned}\mu_{ij}^{v'J'v''J''}&=\langle v'_{J'}|\mu_{ij}(R)|v''_{J''}\rangle\\&=\sum_{k=0}^{N}a_k\langle v'_{J'}|R^k|v''_{J''}\rangle\\&=\langle v'_{J'}|v''_{J''}\rangle\sum_{k=0}^{N}a_k\frac{\langle v'_{J'}|R^k|v''_{J''}\rangle}{\langle v'_{J'}|v''_{J''}\rangle},\end{aligned} \tag{4}$$

where a_k are the desired fitting parameters, while the wave functions (WFs) $|v_J\rangle=\chi_{vJ}(R)$ are the eigenfunctions of the radial Schrödinger equation:

$$\left[-\frac{1}{2m}\frac{d^2}{dr^2}+U^J(R)\right]\chi_{vJ}(R)=E_{vJ}\chi_{vJ}(R). \tag{5}$$

Here m is the reduced molecular mass, $U^J(R)=U_{\rm BO}(R)+[J(J+1)-\Lambda^2]/2mR^2$ is the effective (centrifugally distorted) internuclear potential function, and $U_{\rm BO}(R)$ is the rotationless potential based on the Born–Oppenheimer (BO) separation. The BO potentials can be obtained from direct *ab initio* calculations, as well as from experimental rovibronic level positions either by the semiclassical Rydberg–Klein–Rees (RKR) inversion procedure, or in the framework of a full quantum-mechanical inverted perturbation approach (IPA).[18] In most practical cases the empirical RKR and IPA potentials are essentially more accurate than their *ab initio* counterparts. For this reason, only the empirical potentials have been exploited in the present study since the conventional spectroscopic information (Dunham molecular constants) required for their construction is available for all electronic states under consideration. To solve Eq. (5) numerically, we implemented the iterative renormalized Numerov algorithm[19] combined with the Richardson extrapolation.[20] An efficient phase-matching method was employed to find the eigenvalues.[21] This construction allows one to reduce the absolute errors in rovibrational WFs and in the corresponding overlap integral matrix elements to $10^{-5}-10^{-6}$. The accuracy of the overlap integrals was estimated by calculating the so-called ''noise factors:'' $s_{ij}=|\langle v_i|v_j\rangle|$, where $i\neq j$ and $|v_i\rangle$, $|v_j\rangle$ are vibrational WFs of a given electronic state. The deviation of s_{ij} values from zero is a measure of the nonorthogonality of the calculated WFs.

It is obviously enough to record only one fluorescence progression in order to determine the relative R dependence of the transition dipole moment, whereas τ values for a number of rovibronic v', J' levels are required for the same purpose in case lifetimes are used. At the same time, relative intensities do not allow one to gain the absolute values of the transition moment. From these considerations, the following procedure is usually exploited to determine the $\mu_{ij}(R)$ function. First, by using relative intensities of LIF progression originating from the particular upper rovibronic level, the relative transition moment function is determined, which is subsequently normalized with respect to the experimental lifetime of the v', J' level.[22] Besides, the $\mu_{ij}(R)$ function is

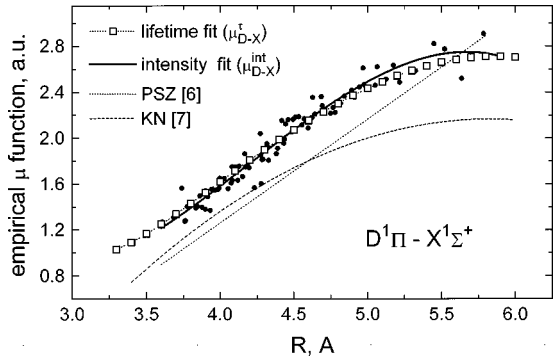

FIG. 2. Empirical $D\,^1\Pi - X\,^1\Sigma^+$ transition dipole moment functions extracted in the present work: (i) $\mu^{\tau}_{D\text{-}X}$ exploiting lifetimes given in Table I; (ii) $\mu^{\rm int}_{D\text{-}X}$—exploiting relative intensities taken from Ref. 6. $\mu(R)$ functions obtained previously by PSZ (Ref. 6) and KN (Ref. 7) are also presented. Closed circles correspond to normalized $\mu^{\rm int}_{D\text{-}X}(R)$ values obtained from corrected PSZ relative intensities data in the framework of the R-centroid approximation (6).

usually expanded in a power series of R [see Eq. (4)], which can be transformed into one-parametric function $\mu_{ij}(R^c)$ using the so-called R-centroid approximation:[23,24]

$$R^k_{v'J'v''J''}=\frac{\langle v'_{J'}|R^k|v''_{J''}\rangle}{\langle v'_{J'}|v''_{J''}\rangle}\approx\left(\frac{\langle v'_{J'}|R|v''_{J''}\rangle}{\langle v'_{J'}|v''_{J''}\rangle}\right)^k=(R^c_{v'J'v''J''})^k. \tag{6}$$

It is this method which has been used by PSZ[6] in order to determine the normalized absolute transition moment function for the $D-X$ transition in NaK as $\mu_{D-X}(R)=-6.0+2.3R$ (μ in debyes, R in angstroms), see the dependence in Fig. 2 labeled as PSZ. It is also worth mentioning that the PSZ $\mu_{D\text{-}X}$ function was later modified by Katô and Noda[7] as $\mu_{D\text{-}X}(R)=-6.0+2.8R-0.24R^2$ (the dependence KN in Fig. 2) in order to describe their relative intensities measured for a single LIF progression which originates from the perturbed $v'=12,J'=7$ $D\,^1\Pi$ state level.

A modified approach has been exploited in the present paper to gain $\mu_{ij}(R)$ from experimental lifetimes and relative intensity data. The essence of the method we are offering here involves the two following steps.

(1) Replacement of exact equation (2) by the approximate expression

$$\tau^{-1}_{iv'J'}\approx\frac{8\pi^2}{3\hbar\epsilon_0}\sum_j\langle v'_{J'}|\Delta U^3_{ij}(R)\mu^2_{ij}(R)|v'_{J'}\rangle, \tag{7}$$

where $\Delta U_{ij}(R)=U_i(R)-U_j(R)$ is the difference potential between i and j electronic states.[25–27] Approximation (7) is based on the additional assumption that the difference potential is independent of J, and $|v'_{J'}\rangle\approx|v'_{J'\pm1}\rangle$, thus allowing one to perform separate summation over v'' and J'' in Eq. (2). As a result, the sum of Hönl–London factors yields $2J'+1$, and the rotational factor in Eq. (7) vanishes.

(2) The simultaneous employment of relative intensities for a number of LIF progressions and lifetime data for the overall set of rovibronic levels in a weighted nonlinear least-squares method (LSM) fitting by means of Eqs. (3) and (7).

Let us stress that the use of the approximate expression (7) practically does not cause any additional inaccuracy in the $\mu_{ij}(R)$ determination since, as was shown by a direct numerical comparison of Eq. (7) with the exact Eq. (2),[27] the relative error of the values obtained by Eq. (7) does not exceed 0.002% for all levels under consideration. Thus, formula (7) can be, in some sense, considered as an ''exact'' one since the accuracy of both lifetime measurements and *ab initio* transition dipole moment calculations are still essentially lower than the accuracy of approximation (7).

The present approach has the following advantages in comparison with the conventional one: (i) Formula (7) avoids the necessity of solving a complete eigenvalue and eigenfunction problem for lower states, being most efficient for distant states and nondiagonal systems. (ii) Formula (7) is much simpler than the exact sum given by Eq. (2), thus allowing one to apply the more stable linear LSM for empirical $\mu_{ij}(R)$ determination from the experimental lifetime values instead of the tedious nonlinear fitting procedure required for the direct application of Eq. (2). (iii) The present approach goes beyond the frame of the R-centroid approximation (6) which, as is known, may cause considerable errors in $\mu_{ij}(R)$ determination, especially when a weak fluorescence band (that is, with small FCF values) is exploited.[24,17]

Since the inversed lifetime (2) is the sum of probabilities of transitions into all lower levels, the individual dipole moment for a transition into a particular state may be obtained explicitly only in two cases: (a) the sum is reduced to a single term, i.e., only a transition into the ground state is possible; (b) the sum is dominated by one strong term, which is likely to occur in cases of comparatively high transition frequency ν_{ij} (since $\tau^{-1}_{iv'J'}$ is proportional to ν^3_{ij}), or in cases when all transitions but one are ''forbidden,'' i.e., they have very small transition probabilities. Thus, strictly speaking, one may use lifetime measurements to normalize the available relative intensity data only if all relative probabilities (branching coefficients) contributing to the sum (2) are known.[28] It is also worth mentioning that experimental lifetimes and relative intensities exploited for determination of the empirical transition dipole moment must correspond to unperturbed levels, otherwise the deperturbation analysis is certainly required before any fitting procedure.[16]

B. $B^1\Pi-X^1\Sigma^+$ transition

The $B\,^1\Pi - X\,^1\Sigma^+$ transition in NaK is a typical example of the present spectroscopic situation when systematic lifetime measurements have been carried out in a wide range of vibrational quantum numbers for the upper state ($1\leqslant v'_B\leqslant 14$, see Fig. 3),[8] while experimental relative intensity data are absent. In this case the empirical $\mu^{\rm em}_{B\text{-}X}(R)$ function can be, in principle, obtained from the lifetime v'_B dependence $\tau(v')$ only. In doing so, we have implemented the approximate relation (7). The required difference potential $\Delta U_{B\text{-}X}(R)=U_{B\,^1\Pi}(R)-U_{X\,^1\Sigma^+}(R)$ has been computed from RKR potentials for $B\,^1\Pi$ and $X\,^1\Sigma^+$ states using the respective molecular constants given in Refs. 29 and 30. Since the experimental $B\,^1\Pi$ state lifetimes correspond to compara-

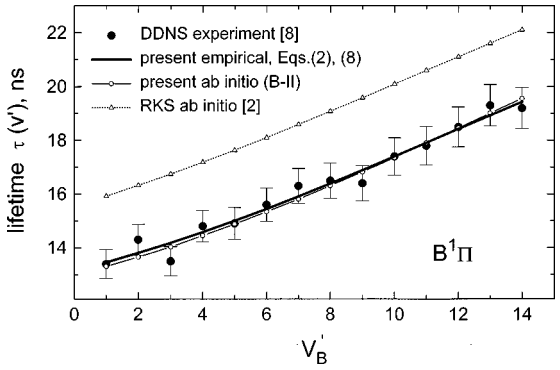

FIG. 3. $B\,^1\Pi$ state lifetimes $\tau(v')$ derived in present work from empirical and *ab initio* $\mu(R)$ functions calculated with larger basis (B-II) set in comparison with experimental data given by DDNS (Ref. 8) for averaged $J'<40$, and with *ab initio* calculations given by RKS (Ref. 2).

tively low J' levels ($J'<40$),[8] most of the lifetimes being averaged over several rotational levels, we have evaluated the expectation values of $\Delta U_{ij}^3(R)R^k$ operators using vibrational WFs corresponding to $J'=30$. Then, the experimental lifetimes given in Ref. 8, along with obtained rovibronic matrix elements, have been processed by a linear LSM procedure in order to obtain the fitting parameters a_k. The singular value decomposition (SVD) of the plan matrix was used to control the linear dependence of the normal equations arising in LSM.[31] The resulting empirical $\mu_{B\text{-}X}^{\rm em}(R)$ function (the bold solid line in Fig. 4) takes the form

$$\mu_{B\text{-}X}^{\rm em}(R)=-4.4428+5.3071R-1.2145R^2+0.0871R^3, \tag{8}$$

with μ in a.u. and R in Å. Equation (8) is valid within the range $3.4\leqslant R(\text{Å})\leqslant 5.8$, which actually corresponds to the interval between the outermost and innermost classical turning points of the highest vibrational $B\,^1\Pi$ state level to be fitted, namely $v_B'=14$. To prove the correctness of the applied inversion procedure, we have recalculated radiative $B\,^1\Pi$ state lifetimes by putting the obtained empirical $\mu_{B\text{-}X}^{\rm em}$ function (8) into the exact equation (2). The result is shown in Fig. 3 (the bold solid line). Note that, although there is one more formally allowed electronic transition from $B\,^1\Pi$ to the lower

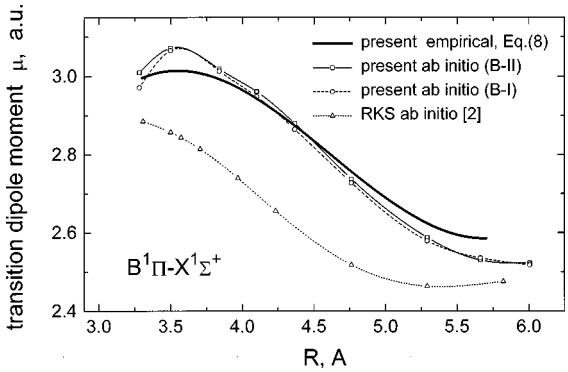

FIG. 4. Empirical $B\,^1\Pi-X\,^1\Sigma^+$ transition dipole moment functions $\mu_{B\text{-}X}(R)$ and their *ab initio* calculations with smaller basis (B-I) and larger basis (B-II) accomplished in the present work in comparison with *ab initio* calculations performed by RKS (Ref. 2).

lying $A^1\Sigma^+$ state, its contribution into the $B\,^1\Pi$ state lifetime values is negligible due to both frequency and probability factors, since $\nu_{B\text{-}A}^3 \ll \nu_{B\text{-}X}^3$ and $\mu_{B\text{-}A}^2 \ll \mu_{B\text{-}X}^2$.[2]

C. $D^1\Pi-X^1\Sigma^+$ transition

The following distinctions between $D\,^1\Pi-X\,^1\Sigma^+$ and $B\,^1\Pi-X\,^1\Sigma^+$ systems should be pointed out concerning the empirical determination of transition dipole moments.

(1) In addition to lifetime measurements, the experimental relative intensities in the $D\,^1\Pi\rightarrow X\,^1\Sigma^+$ LIF spectrum originating from a particular $D\,^1\Pi v',J'$ level are available from PSZ data.[6]

(2) Lifetime and relative intensity measurements have been carried out for a number of v',J' levels, without any averaging over J', including very high J' values ($J'\sim 100$, see Table I) for which it is necessary to take into account the effect of rotation on vibrational WFs and corresponding matrix elements.

(3) Some levels under study can be locally perturbed by the close lying $d\,^3\Pi$ state due to intramolecular spin–orbit interaction,[14,32] which means that the corresponding experimental lifetimes and relative intensities can differ from the ''true'' ones. Indeed, as was shown in Ref. 14, the $v'=11,J'=46$ and $v'=12,J'=7$ levels are certainly perturbed and experimentally measured lifetimes for these levels have therefore been excluded from the fitting. It has to be added, however, that, in obtaining empirical $D-X$ transition dipole moment functions, we have completely ignored the branching ratio coefficients, that is the ratios of singlet bound–bound $D\,^1\Pi\rightarrow X\,^1\Sigma^+$ and triplet bound–free $d\,^3\Pi\rightarrow a\,^3\Sigma^+$ transitions for the $D\,^1\Pi$ state levels $v'=1,J'=67$; $v'=7,J'=23$ and $v'=10,J'=102$, see Table III from Ref. 6. PSZ[6] supposed that the above levels are considerably mixed with the $d\,^3\Pi$ state levels. To clarify this point, we have estimated the mixing coefficients for these levels using experimental deperturbed molecular constants of the perturbing $d\,^3\Pi$ state and corresponding nondiagonal spin–orbit electronic matrix elements given in Ref. 32. These calculations confirmed for us that the $D\,^1\Pi$ state v',J' levels under discussion are practically not perturbed by the $d\,^3\Pi$ state in contrast to the $v'=11,J'=46$ and $v'=12,J'=7$ levels mentioned above. Therefore, the transition probabilities into the triplet continuum given in Table III of Ref. 6 seem to have to be attributed to the bound–free LIF spectrum arising from other strongly perturbed $D\,^1\Pi$ levels excited by the same laser line (see Tables II and VII in Ref. 15).

(4) The $D\,^1\Pi\rightarrow A\,^1\Sigma^+$ transition can, in general, contribute to $D\,^1\Pi$ lifetime values. This contribution has been estimated by exploiting Eq. (7) and the *ab initio* $\mu_{D\text{-}A}(R)$ function (see Table II; the calculations will be described in detail in Sec. IV). The difference $\Delta U_{D\text{-}A}(R)=U_{D\,^1\Pi}(R)-U_{A^1\Sigma^+}(R)$ has been obtained using the $D\,^1\Pi$ state IPA potential represented in Table VIII of Ref. 15 and the $A\,^1\Sigma^+$ state RKR potential derived from the molecular constants given in Ref. 33. The obtained $D-A$ transition probabilities $A_{D\text{-}A}$ (Table III) make a small but non-negligible contribution in the $D\,^1\Pi$ state lifetimes. This contribution should therefore be subtracted from the inversed experimental life-

TABLE II. *Ab initio* finite-field MPPT transition dipole moment functions obtained with the two atomic basis sets (B-I and B-II).

	$\mu(R)$ (a.u.)					
	$D\,^1\Pi - X\,^1\Sigma^+$		$B\,^1\Pi - X\,^1\Sigma^+$		$D\,^1\Pi - A\,^1\Sigma^+$	
R(Å)	B-I	B-II	B-I	B-II	B-I	B-II
3.281	1.275	1.214	2.971	3.009	1.574	1.652
3.498	1.220	1.227	3.065	3.072	1.597	1.597
3.837	1.470	1.464	3.014	3.019	1.417	1.456
4.101	1.696	1.680	2.949	2.961	1.285	1.317
4.366	1.929	1.910	2.865	2.880	1.127	1.163
4.763	2.247	2.242	2.728	2.738	0.897	0.942
5.292	2.565	2.561	2.579	2.588	0.620	0.659
5.662	2.699	2.701	2.535	2.530	0.483	0.516
6.006	2.772	2.771	2.515	2.522	0.353	0.375

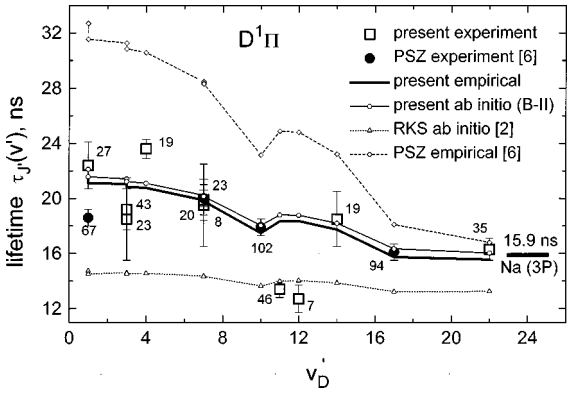

FIG. 5. Experimentally measured NaK $D\,^1\Pi$ state rovibrational lifetimes $\tau_{J'}(v')$, their calculated empirical values obtained using empirical $\mu^{\rm em}_{D\text{-}X}(R)$ functions given in present work (present empirical) and in Ref. 6 (PSZ empirical). The *ab initio* lifetime calculations obtained in present work with basis II (present *ab initio*) and given in Ref. 2 (RKS *ab initio*) are also depicted. Numbers denote J' values of the levels under study.

times gained from Table I in order to get, by means of the fitting procedure, the empirical $\mu_{D\text{-}X}(R)$ function corresponding to the D-X transition only. The remaining allowed $D\,^1\Pi \rightarrow B\,^1\Pi$ and $D\,^1\Pi \rightarrow C\,^1\Sigma^+$ transitions contribute practically nothing in $D\,^1\Pi\,\tau(v',J')$ values owing to very small frequency and electronic probability factors, since $\nu^3_{D\text{-}C} \ll \nu^3_{D\text{-}B} \ll \nu^3_{D\text{-}X}$ and $\mu^2_{D\text{-}C} \ll \mu^2_{D\text{-}B} \ll \mu^2_{D\text{-}X}$.[2]

To check the self-consistency of experimental lifetime and relative intensity data we have exploited them independently of each other in order to obtain, in two different ways, the empirical $\mu(R)$ functions for the same $D-X$ transition. First, the $D\,^1\Pi(v',J')$ state lifetime with values measured in the present work from rf-ODR contours (the open squares in Fig. 5), along with the PSZ[6] lifetimes measured from fluorescence decay kinetics (the closed circles in Fig. 5), have been processed by the weighted linear LSM making use of Eq. (7). The resulting empirical function $\mu^{\tau}_{D\text{-}X}(R)$ is depicted in Fig. 2 (open squares). Second, the relative intensities of the $D\,^1\Pi(v',J') \rightarrow X\,^1\Sigma^+(v'',J'')$ LIF spectrum presented in Tables I and II of Ref. 6 have been fitted in accordance with Eq. (3) by linear LSM in order to determine the relative transition dipole moment function $\mu^{\rm int}_{D\text{-}X}(R)$. The required rovibrational WFs for $D\,^1\Pi$ and $X\,^1\Sigma^+$ states have been obtained by the numerical solution of Eq. (5) with the corresponding effective potentials. Note that, as distinct from PSZ,[6] in the course of exploiting their data we have used the correct *cubic* relative intensity dependence on transition frequency ν, that is, taking $n=3$ in Eq. (3) instead of $n=4$. This correction is based upon the fact that intensity measurements in Ref. 6 have been performed by detecting the *numbers of photon counts* using the photon counting regime. Besides, we have exploited the $X\,^1\Sigma^+$ state RKR potential based upon essentially improved molecular constants,[30] which is of particular importance for large v',J' and v'',J'' values. The relative $\mu^{\rm int}_{D\text{-}X}(R)$ function has been scaled to the absolute $\mu^{\tau}_{D\text{-}X}(R)$ function discussed above. It is easy to see from Fig. 2 that the normalized $\mu^{\rm int}_{D\text{-}X}(R)$ function (the solid line) is in good agreement with its lifetime counterpart $\mu^{\tau}_{D\text{-}X}(R)$. As it also follows clearly from Fig. 2, both functions go steeply toward the value of the transition dipole moment between $3P$ and $3S$ states of the Na atom (2.52 $\pm$0.04 a.u.[34]), which is exactly what should be expected if one remembers that the interacting $D\,^1\Pi$ and $X\,^1\Sigma^+$ states dissociate into $(3P)$Na+$(4S)$K and $(3S)$Na+$(4S)$K atomic limits, respectively. At the same time, the present functions are significantly different from the PSZ[6] and KN[7] empirical functions. The above discussion allows us to suppose that the present empirical $\mu^{\rm int}_{D\text{-}X}(R)$ and $\mu^{\tau}_{D\text{-}X}(R)$ functions are more reliable than the dependencies presented by PSZ[6] and KN.[7] Finally, the relative intensities for four progressions given by PSZ,[6] along with lifetimes data for the overall set of rovibronic levels given in Table I, have been processed simultaneously by a weighted nonlinear LSM fitting procedure exploiting Eqs. (3) and (7), yielding the following unified empirical $D\,^1\Pi - X\,^1\Sigma^+$ transition dipole moment function ($\mu^{\rm em}_{D\text{-}X}$ in a.u., R in Å):

$$\mu^{\rm em}_{D\text{-}X}(R) = 4.1610 - 3.6822R + 1.1280R^2 - 0.0919R^3, \tag{9}$$

TABLE III. Radiative NaK $D\,^1\Pi(v',J')$ state lifetimes (in ns) calculated by Eq. (7) with empirical potential curves using the following $D\,^1\Pi - X\,^1\Sigma^+$ transition dipole moment functions: (a) empirical, obtained in the present work ($\tau^{\rm present}_{\rm em}$) or given by PSZ—Ref. 6 ($\tau^{\rm PSZ}_{\rm em}$) and KN—Ref. 7 ($\tau^{\rm KN}_{\rm em}$); (b) *ab initio* calculated in the present work (FF-MPPT, $\tau^{\rm present}_{\rm ab}$) or given by RKS—Ref. 2 (pseudopotential, $\tau^{\rm RKS}_{\rm ab}$). The *ab initio* FF-MPPT $D\,^1\Pi - A\,^1\Sigma^+$ transition probabilities $A_{D\text{-}A}$ (in $10^6\ s^{-1}$) calculated in the present work are also presented.

v'	J'	$\tau^{\rm present}_{\rm em}$	$\tau^{\rm present}_{\rm ab}$	$\tau^{\rm PSZ}_{\rm em}$	$\tau^{\rm KN}_{\rm em}$	$\tau^{\rm RKS}_{\rm ab}$	$A_{D\text{-}A}$
1	27	22.5	23.0	34.5	31.2	15.1	1.631
1	67	21.8	22.3	33.2	30.3	14.9	1.572
3	23	21.8	22.2	32.9	30.7	14.9	1.574
3	43	21.6	22.0	32.4	30.4	14.9	1.553
4	19	21.5	21.8	32.1	30.4	14.9	1.546
7	8	20.5	20.8	29.7	29.6	14.7	1.458
7	20	20.4	20.8	29.6	29.5	14.6	1.453
7	23	20.4	20.8	29.5	29.5	14.6	1.450
10	102	17.8	18.4	23.8	26.7	13.9	1.184
11	46	18.8	19.3	25.7	28.1	14.2	1.294
12	7	18.8	19.3	25.6	28.2	14.3	1.296
14	19	18.1	18.6	23.9	27.6	14.1	1.222
17	94	16.0	16.6	18.4	25.2	13.4	0.948
22	35	15.8	16.3	17.1	25.5	13.4	0.904

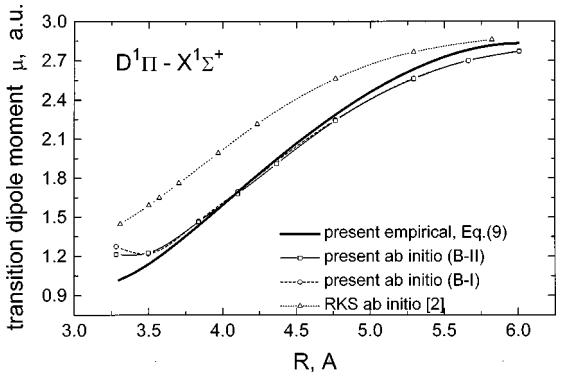

FIG. 6. Empirical and *ab initio* $D\,^1\Pi - X\,^1\Sigma^+$ transition dipole moment functions $\mu_{D\text{-}X}(R)$.

which is reliable within the range $3.3<R(\text{Å})<6.0$ (the bold solid line in Fig. 6).

IV. *AB INITIO* CALCULATIONS

The transition dipole moment functions have been computed using the finite-field (FF) technique[35–37] which is known as an efficient tool for *ab initio* studies of electric properties of molecules in pure electronic states. The generalization of the FF technique for transition property calculations is rather straightforward and can be briefly presented as follows. A molecule placed in external uniform electric field with intensity F is described by the Hamiltonian

$$H=H(F)=H(0)-\mu F, \tag{10}$$

where $H(0)$ denotes the Hamiltonian of the free molecule and $\mu=-(\partial H/\partial F)$ is the conventional electric dipole operator. Exact F-dependent eigenfunctions Ψ_i, Ψ_j and eigenvalues E_i, E_j of H should satisfy the off-diagonal Hellmann–Feynman relation:

$$\langle\Psi_i|\mu|\Psi_j\rangle=(E_i-E_j)\left\langle\Psi_i\left|\frac{\partial\Psi_j}{\partial F}\right.\right\rangle. \tag{11}$$

The central two-point finite-difference approximation for the derivative on the right-hand side of Eq. (11) at $F=0$ provides the following working formula of the FF method for the transition moment in a free molecule:

$$(\mu_{ij}^{\text{FF}})_\eta\approx(E_i-E_j)\langle\Psi_i(F_\eta=-\Delta/2)|\Psi_j(F_\eta=\Delta/2)\rangle/\Delta,$$
$$\eta=x,y,z, \tag{12}$$

where Δ is a numerical differentiation step size. Since Eq. (11) generally does not hold for approximate wave functions (WFs) resulting from practical *ab initio* calculations, the estimate (12) can differ from the corresponding off-diagonal electric dipole matrix element (dipole length form of the transition moment) computed with the same approximate electronic WFs. As has been demonstrated recently,[38] the FF results are normally more stable with respect to the level of electronic correlation treatment than their dipole-length analogs. This advantage of the FF technique seems to overcome its evident drawbacks which consist of limited numerical accuracy because of rounding errors for small Δ and significant nonlinear contributions when Δ is large, as well as the necessity to perform at least two series of calculations with different F values. One should also realize that the external field can lower the symmetry of the system under study, thus giving rise to additional computational work. For instance, the FF calculations on the $\Sigma-\Pi$ transition moments in NaK should be performed in C_s symmetry, and the states involved in the transitions have the same symmetry (A') in the presence of an external field.

A quantitative *ab initio* description of excited electronic states of NaK requires an adequate reproduction of complicated valence configuration mixing strongly affected by the core-valence correlations. At the all-electron level of the theory, this implies the necessity to correlate a rather large number of electrons (including at least outer core shells of both atoms) within an inherently multiconfigurational (i.e., multireference) approach. In the present study the calculations of the WFs in the finite field were carried out by the many-body multipartitioning perturbation theory (MPPT).[9] With an appropriate choice of model (reference) space, this approach may take advantage of the physically grounded separation of electron correlation effects into valence and core-valence correlations, properly taking into account their interplay. Offering the possibilities to maintain strict size consistency and to treat vast model spaces without any risk of instabilities caused by intruder states, the second-order MPPT appears to be ideally suited to our task.

We used a recently developed MPPT code[39] interfaced to the MOLCAS suite of programs for electronic structure calculations.[40] Two basis sets were employed in our study. The smaller one, $(14s10p4d1f)/[7s5p3d1f]$Na, $(15s13p4d1f)/[9s7p3d1f]$K (hereafter referred as B-I) was obtained from the standard basis for electric property calculations[41] by decontracting the outermost d functions and adding the f functions with exponential parameters 0.06(Na) and 0.04(K). The larger one, referred as B-II, comprised additional single sets of diffuse s, p and d functions (exponential parameters 0.0033, 0.0019, 0.016 and 0.0025, 0.0013, 0.007 for Na and K, respectively), however the original contraction of the d shell proposed in Ref. 41 was restored. Orthogonal molecular orbitals were generated by solving the state-average self-consistent field (SCF) problem for the two lowest $^2\Sigma^+$ states of NaK^+. The model space for MPPT calculations with B-I basis was the full valence configuration-interaction space, or, in other words, it comprised the configurations with doubly occupied core molecular orbitals and all possible arrangements of two valence electrons among the valence and virtual orbitals. When the larger basis (B-II) was used, we had to restrict the model space size to ~500, omitting the valence configurations with negligible contributions to the WFs of interest. This choice of model spaces guarantees a strict (B-I) or a very good approximate (B-II) size consistency of results. Within the model space, we have constructed a state-selective Hermitian effective Hamiltonian[9,42] with five $^1A'$ target states which corresponded to the three lowest Σ and two Π singlet states of the free molecule. The effective Hamiltonian incorporated the core-valence correlation and core polarization effects at the second order in MPPT. At the perturbation step the in-

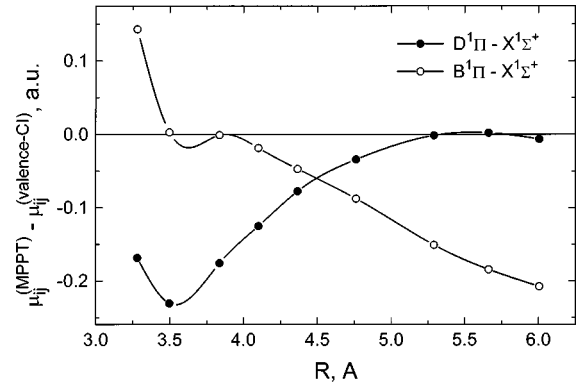

FIG. 7. Core-valence correlation effects upon calculated transition dipole moments.

nermost core orbitals $1s$(Na), $1s2s2p$(K) were frozen, i.e., 18 electrons were explicitly correlated.

The external electric field intensities corresponded to the step size $\Delta=10^{-4}$ a.u.; additional calculations with Δ values in the range $10^{-5}\leqslant\Delta\leqslant 2\times10^{-4}$ a.u. provided the μ_{ij}^{FF} estimates which were stable within 10^{-3} a.u. The overlap integrals entering the FF formula (12) for transition dipole moments have been evaluated with the valence eigenfunctions obtained by diagonalizing the effective Hamiltonian. Although the direct contributions to these integrals from core-excited configurations were thus ignored, the use of the FF scheme allowed us to incorporate implicitly the corresponding contributions into transition moment estimates (see the Appendix). Moreover, owing to the ''perturb-then-diagonalize'' strategy realized in our approach, the influence of core-valence correlations on μ_{ij}^{FF} values via correlation interference effects[43,44] was fully taken into account. The importance of core-valence correlation effects are demonstrated by the comparison of MPPT transition moments with the full valence CI ones in Fig. 7. Notice that the popular polarization pseudopotential technique[1,2,45] gives a less adequate description of these effects since: (1) the two-particle effective interactions of valence electrons arising from core-valence correlations cannot be properly fitted by any one-particle pseudopotential; (2) the direct contributions from core-excited configurations to any property other than the energy are completely ignored; (3) the spurious contributions to transition moments arising from nonorthogonality of valence pseudo-WFs to the core, in contradistinction with similar contributions to the total energy, are not automatically countervailed. The high accuracy of the transition moments for free non-valence-electron atoms computed by the pseudopotential method[2] imply that the two latter factors should not be of crucial importance. In contrast, the effective two-particle interactions in the valence shell can affect the valence part of the WFs and therefore the characteristics of valence transitions.

The resulting $B\,^1\Pi-X\,^1\Sigma^+$ and $D\,^1\Pi-X\,^1\Sigma^+$ transition dipole moment functions are presented in Table II and plotted in Figs. 4 and 6, respectively. Let us first note that the μ_{ij} estimates obtained with two different bases (B-I and B-II) are almost identical. The discrepancy exceeds 1% only for the $D-X$ transition at very short internuclear distance ($R\leqslant3.5$ Å). The $\mu_{B\text{-}X}$ and $\mu_{D\text{-}X}$ *ab initio* data closely fit the corresponding empirical transition moment functions obtained in Sec. III. Unfortunately, the accuracy of the computed $D\,^1\Pi-A\,^1\Sigma$ transition moment (Table II) cannot be directly estimated from the available experimental data since intensity measurements of the $D\,^1\Pi-A\,^1\Sigma$ transition are absent and the contribution of the $D\,^1\Pi\rightarrow A\,^1\Sigma$ channel to the radiative decay of the $D\,^1\Pi(v',J')$ levels is rather small (Table III). It is worth noting the qualitative agreement of our transition moment functions with the RKS data; quantitative differences can be explained by the simplified treatment of core-valence correlations and the use of rather restricted valence basis sets in the pseudopotential calculations.[2] The relative strengths of the remaining allowed transitions $D\,^1\Pi-B\,^1\Pi$, $D\,^1\Pi-C\,^1\Sigma^+$ and $B\,^1\Pi-A\,^1\Sigma^+$ have also been obtained in the course of the present *ab initio* calculations in order to estimate their contributions to radiative lifetimes of $D\,^1\Pi$ and $B\,^1\Pi$ states, respectively.

V. LIFETIME CALCULATIONS

The present empirical and MPPT *ab initio* $\mu_{D\text{-}X}(R)$ functions, as well as those from pseudopotential *ab initio* calculations of RKS[2] and empirical functions given by PSZ[6] and KN[7] have been exploited to calculate $D\,^1\Pi$ state lifetimes by using Eq. (7) and empirical potentials. The results are presented in Table III. The corresponding $\tau_{v',J'}$ values corrected by accounting for the $D-A$ transition contribution (see Table III) are plotted in Fig. 5. One can see that both FF MPPT and empirical function $\mu_{D\text{-}X}(R)$ (9) allow one to reproduce the experimental lifetimes significantly better than the RKS[2] and the empirical PSZ[6] and KN[7] $\mu(R)$ functions. The $B\,^1\Pi(v')$ state radiative lifetimes $\tau_{v'}$ derived from the present *ab initio* transition dipole moments and empirical potential curves quantitatively reproduce the experimental values as well (Fig. 3). It should be emphasized that an improvement over the results of RKS[2] pseudopotential calculations was gained for the lifetimes of both electronic states under study.

As it was already shown, the introduction of a centrifugal distortion term into the effective potential $U^J(R)$ in Eq. (5) is definitely required to properly take into account the rotation effect on vibrational WFs for high J' levels, since the rotation effect can dramatically change the magnitude of small rovibronic matrix elements (4) corresponding to small Franck–Condon factors $|\langle v'_{J'}|v''_{J''}\rangle|^2$.[17] Obviously, the rotation effect has to cause lifetime variation with rotational quantum number J'. Indeed, under the simplest harmonic approximation, the lifetime J' dependence for a given vibrational level v' can be expressed by means of Eq. (7) in the following analytical form:

$$\tau_{iv'J'}\approx\tau_{iv'}(1-\gamma_i[J'(J'+1)-\Lambda^2]), \tag{13}$$

$$\gamma_i=\left(\frac{2B_{ei}}{\omega_{ei}}\right)^2 R_{ei}\left[\sum_j \frac{2\mu'_{ij}(R_{ei})}{\mu_{ij}(R_{ei})}-\frac{m\omega_{ei}^2}{11.238}\sum_j\frac{R_{ei}-R_{ej}}{T_{ei}-T_{ej}}\right], \tag{14}$$

where the reduced mass m is in Aston units,[46] equilibrium distances R_{ei}, R_{ej} are in Å, while electronic energies

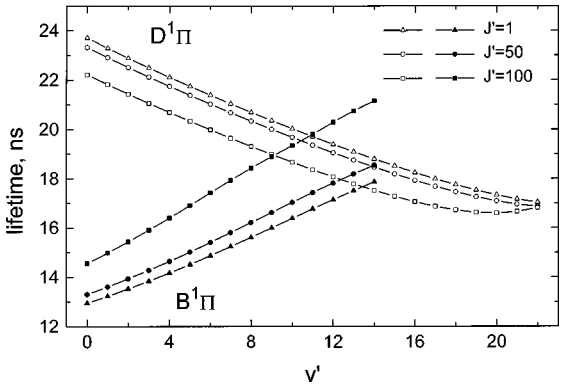

FIG. 8. Rotational effect on radiative lifetimes of $B\,^1\Pi$ and $D\,^1\Pi$ states.

T_{ei}, T_{ej}, rotational (B_{ei}) and vibrational (ω_{ei}) molecular constants are in cm^{-1}. The $\mu'_{ij}(R_{ei}) \equiv d\mu_{ij}/dR$ denotes the first derivative of the dipole moment function $\mu_{ij}(R)$ with respect to internuclear distance R. Relations (13) and (14) demonstrate that the lifetime J dependence should be most pronounced for long living states corresponding to small $\nu_{ij} = T_{ei} - T_{ej}$ and small μ_{ij} factors, as well as for the nondiagonal systems (with large $\Delta R_e = R_{ei} - R_{ej}$ values) possessing pronounced R dependence of the dipole moment function (large $d\mu_{ij}/dR$).

To estimate the rotation effect upon the lifetimes of the $B\,^1\Pi$ and $D\,^1\Pi$ states, we have evaluated the corresponding γ_i parameters in Eq. (14) by using respective molecular constants and empirical $B-X$ and $D-X$ transition dipole moment functions. The γ values obtained ($\gamma_{B\,^1\Pi} = -8.3 \times 10^{-6}$, $\gamma_{D\,^1\Pi} = 7.2 \times 10^{-6}$) mean that $\tau(B\,^1\Pi)$ has to increase as J' increases, while $\tau(D\,^1\Pi)$ has to decrease as J' increases. Indeed, for the $D\,^1\Pi$ state an ''unexpected'' minimum can be distinguished in Fig. 5 upon the relatively smooth v' dependence of both experimental and calculated lifetime values. This minimum corresponds to a rovibronic level with maximal J' value under study, namely $J' = 102$. Hence, we can suppose that it is the rotation effect which is responsible for the lifetime decrease. To check this point, we have calculated $\tau(D\,^1\Pi)$ and $\tau(B\,^1\Pi)$ for lowest ($J' = 1$), medium ($J' = 50$) and high ($J' = 100$) J' values. The results obtained are represented in Fig. 8 and completely confirm the above statements. Moreover, a linear fit of the calculated $\tau(v', J')$ values for the lowest v' values yields γ_i parameters $\gamma_{B\,^1\Pi} = -12.1 \times 10^{-6}$ and $\gamma_{D\,^1\Pi} = 6.6 \times 10^{-6}$, being in good agreement with those obtained above within the harmonic approximations (13) and (14). The obtained $\gamma_{D\,^1\Pi}$ values allow one to explain the diminution of the experimental $D\,^1\Pi$ lifetimes for high J levels, namely $\tau_{v'=10}(J' = 102) = 17.9$ ns and $\tau_{v'=17}(J' = 94) = 16.1$ ns, see Table I. Indeed, at $J' = 1$ our lifetime calculations for these levels performed with semiempirical transition moments yielded larger values, namely $\tau_{v'=10}(J' = 1) = 19.3$ ns and $\tau_{v'=17}(J' = 1) = 17.1$ ns. At the same time, Eq. (13) with $\gamma_{D\,^1\Pi} = 6.6 \times 10^{-6}$ gives the values $\tau_{v'=10}(J' = 102) = 18.0$ ns and $\tau_{v'=17}(J' = 94) = 16.2$ ns which agree with the experimental results. Thus, the rotation effect leads to a noticeable ($\approx$1.5–2.0 ns) contribution to the lifetimes of high J' levels for both states under study. As is well known, the probability densities of rovibrational WFs shift smoothly to the right along the R axis as v' and J' increase. This leads to a situation when $\chi^2_{v'J'}(R)$ functions for two different rovibronic levels (v'_1, J'_1) and (v'_2, J'_2), belonging to the same electronic state, can be localized predominantly in the same relatively narrow R region if the following conditions are fulfilled simultaneously: $v'_2 > v'_1 \gg 1$ and $J'_2 \ll J'_1$. This means that the integrand functions $\Delta U^3_{ij}(R)\mu^2_{ij}(R)\chi^2_{vJ}(R)$ for these levels, along with the corresponding lifetime values, should be close to each other in case of any smooth dipole moment function $\mu_{ij}(R)$. This is the reason why, for instance, $\tau_{J'=102}(v' = 10) \approx \tau_{J'=19}(v' = 14)$ and $\tau_{J'=94}(v' = 17) \approx \tau_{J'=35}(v' = 22)$ for the $D\,^1\Pi$ state (Table III).

VI. CONCLUSIONS

Excellent agreement between *ab initio* and empirical $B\,^1\Pi - X\,^1\Sigma^+$ and $D\,^1\Pi - X\,^1\Sigma^+$ transition dipole moment functions obtained in the framework of the present approaches has been achieved.

A possibility has been demonstrated allowing one to determine the absolute transition dipole moment function $\mu(R)$, in wide R range, by means of the approximate relation (7) and the experimental data on lifetime variations with vibrational and rotational quantum numbers. The approach was employed successfully to describe the $B\,^1\Pi - X\,^1\Sigma^+$ transition in which relative intensity data are absent. Satisfactory agreement between the results obtained applying Eq. (7) and the ones gained from the relative intensities by applying Eq. (3) with $n = 3$ has been achieved in the case of $D\,^1\Pi - X\,^1\Sigma^+$ transition.

The empirical $D\,^1\Pi - X\,^1\Sigma^+$ transition dipole moment function $\mu(R)$ has been improved considerably by means of: (a) extension of the (v', J') range of the experimental lifetime data; (b) corrected description of relative intensities measured by the photon-counting regime [$n = 3$ in Eq. (3)]; (c) simultaneous fitting of lifetime and relative intensity data; (d) taking into account implicitly the J' dependence of experimental lifetime values in fitting procedures.

The combination of the finite-field (FF) technique and many-body multipartitioning perturbation theory (MPPT) has been shown to be adequate for obtaining reliable transition dipole moment values owing to a proper description of the core-valence correlation contributions into transition moment estimates.

ACKNOWLEDGMENTS

Financial support for this work by the Russian Foundation of Basic Research under Grant Nos. 97-03-32215a and 97-03-33714a is gratefully acknowledged by three of us (E.P., A.S., and A.Z.). A.Z. thanks Professor Björn O. Roos for supplying him with the MOLCAS 3 package. This work was supported by the European Commission in the frame of PECO Human Capital and Mobility (Network) LAMDA program, Contract No. ERBCIPDCT940633, and we are especially indebted to Dr. Henrik Rudolph and Dr. Henk Dijkerman for their constant efforts to help us in carrying out the project. The Riga group participants have been supported by the Latvian Science Council (Grant No. 96.0323). Support

by the research group ''Interaction of Oriented Molecules'' of the Center for Interdisciplinary Research (ZiF) at the University of Bielefeld is gratefully acknowledged by one of us (M.A.). We are especially grateful to graduate student Janis Alnis for his considerable help in fixing the setup and participation in measurements.

APPENDIX

Let us assume that the basis configuration state functions do not depend on the field intensity F. In the present study this is ensured by the use of nonrelaxed molecular orbitals of the free ($F=0$) NaK^+ ion in the calculations on NaK for any field intensity. Denoting the model-space and outer-space basis functions by $|m\rangle,|n\rangle \ldots$ and $|a\rangle,|b\rangle \ldots$, respectively, and introducing the model-space projector $P=\Sigma_m|m\rangle\langle m|$ which is also independent of F, we can write down the F-dependent second-order Hermitian effective Hamiltonian in the form:

$$H_{\mathrm{eff}}^{[2]}(F)=PH(F)P+\frac{1}{2}\sum_{mn}\sum_{a}|m\rangle H_{ma}(F)\times\left(\frac{1}{D_{ma}}+\frac{1}{D_{na}}\right)H_{an}(F)\langle n|. \tag{A1}$$

Here D_{ma}, D_{na} are the energy denominators defined by the MPPT manifold of zero-order Hamiltonians (see Ref. 9 for explicit formulas). For the sake of simplicity, we shall suppose that these entities are F independent, i.e., that MPPT zero-order Hamiltonians constructed for $F=0$ are further used in the second-order calculations for nonzero field intensities. If calculations for different F values are performed separately, neglecting the F dependence of the energy denominators is a reasonable approximation. Substituting the expression for the field-dependent total Hamiltonian (10) into Eq. (A1) and regrouping the terms according to their powers in F, one gets:

$$H_{\mathrm{eff}}^{[2]}(F)=H_{\mathrm{eff}}^{[2]}(0)-FM+O(F^2), \tag{A2}$$

where

$$M=P\mu P+\frac{1}{2}\sum_{mn}\sum_{a}|m\rangle(H_{ma}(0)\mu_{an}+\mu_{ma}H_{an}(0))\times\left(\frac{1}{D_{ma}}+\frac{1}{D_{na}}\right)\langle n|. \tag{A3}$$

Obviously,

$$M=-\left.\frac{\partial H_{\mathrm{eff}}^{[2]}}{\partial F}\right|_{F=0}. \tag{A4}$$

One easily notices that Eq. (A3) resembles the expression for the first-order effective electric dipole operator:[47,48]

$$\mu_{\mathrm{eff}}^{[1]}=P\mu P+\sum_{mn}\sum_{a}|m\rangle\times\left(\frac{H_{ma}(0)\mu_{an}}{D_{ma}}+\frac{\mu_{ma}H_{an}(0)}{D_{na}}\right)\langle n|. \tag{A5}$$

Provided that $|D_{ma}-D_{na}|\ll|D_{ma}|$ (this requirement is normally satisfied at least for model space configurations $|m\rangle$, $|n\rangle$ with large weights in the target vector expansions), the M matrix elements between the target states should approach the corresponding $\mu_{\mathrm{eff}}^{[1]}$ matrix elements:

$$\langle\tilde{\Psi}_i|M|\tilde{\Psi}_j\rangle\cong\langle\tilde{\Psi}_i|\mu_{\mathrm{eff}}^{[1]}|\tilde{\Psi}_j\rangle. \tag{A6}$$

Since $\mu_{\mathrm{eff}}^{[1]}$ is Hermitian, its eigenfunctions $\tilde{\Psi}_i$, $\tilde{\Psi}_j$, $i\neq j$ satisfy

$$\langle\tilde{\Psi}_i|\tilde{\Psi}_j\rangle=0,\ \langle\tilde{\Psi}_i|H_{\mathrm{eff}}^{[2]}|\tilde{\Psi}_j\rangle=0. \tag{A7}$$

Differentiating Eq. (A7) with respect to field intensity and taking into account Eq. (A4), one readily arrives at a Hellmann–Feynman-like relation

$$(E_i-E_j)\left\langle\tilde{\Psi}_i\left|\frac{\partial\tilde{\Psi}_j}{\partial F}\right\rangle\right|_{F=0}=\langle\tilde{\Psi}_i|M|\tilde{\Psi}_j\rangle\cong\langle\tilde{\Psi}_i|\mu_{\mathrm{eff}}^{[1]}|\tilde{\Psi}_j\rangle. \tag{A8}$$

Although the functions $\tilde{\Psi}_i,\tilde{\Psi}_j$ are restricted to the model space and do not comprise any contributions from outer-space (core-excited) configurations, Eq. (A8) clearly indicates that FF transition dipole moment estimates computed with these functions implicitly incorporate the bulk of such contributions entering the first-order effective electric dipole operator (A5). To achieve a similar level of accuracy with the dipole-length formula, one should explicitly construct the first-order effective operator (A5) or, equivalently, evaluate the outer-space part of the WFs using first-order wave operator.[9,47,48]

[1] S. Magnier and Ph. Millie, Phys. Rev. A **54**, 204 (1996).
[2] L. B. Ratcliff, D. D. Konowalow, and W. J. Stevens, J. Mol. Spectrosc. **110**, 242 (1985).
[3] M. M. Hessel, E. W. Smith, and R. E. Drullinger, Phys. Rev. Lett. **33**, 1251 (1974).
[4] W. Demtröder, W. Stetzenbach, M. Stock, and J. Witt, J. Mol. Spectrosc. **61**, 382 (1976).
[5] W. J. Stevens, M. M. Hessel, P. J. Bertoncini, and A. C. Wahl, J. Chem. Phys. **66**, 1477 (1977).
[6] J. Pfaff, M. Stock, and D. Zevgolis, Chem. Phys. Lett. **65**, 310 (1979).
[7] H. Katô and C. Noda, J. Chem. Phys. **73**, 4940 (1980).
[8] J. Derouard, H. Debontride, T. D. Nguyen, and N. Sadeghi, J. Chem. Phys. **90**, 5936 (1989).
[9] A. Zaitsevskii and J. P. Malrieu, Theor. Chim. Acta **96**, 269 (1997), and references therein.
[10] S. J. Silvers, T. H. Bergeman, and W. Klemperer, J. Chem. Phys. **52**, 4385 (1970).
[11] R. W. Field and T. H. Bergeman, J. Chem. Phys. **54**, 2936 (1971).
[12] R. E. Drullinger, M. M. Hessel, and E. W. Smith, in *Laser Spectroscopy*, edited by S. Haroche *et al.* (Springer, Berlin, 1975), p. 91.
[13] M. Tamanis, M. Auzinsh, I. Klincare, O. Nikolayeva, A. V. Stolyarov, and R. Ferber, J. Chem. Phys. **106**, 2195 (1997).
[14] M. Tamanis, M. Auzinsh, I. Klincare, O. Nikolayeva, R. Ferber, E. A. Pazyuk, A. V. Stolyarov, and A. Zaitsevskii, Phys. Rev. A **58**, 1932 (1998).
[15] M. M. Hessel and S. Giraud-Cotton (unpublished).
[16] H. Lefebvre-Brion and R. W. Field, *Perturbations in the Spectra of Diatomic Molecules* (Academic, New York, 1986).
[17] Ya. A. Harya, R. S. Ferber, N. E. Kuz'menko, O. A. Shmit, and A. V. Stolyarov, J. Mol. Spectrosc. **125**, 1 (1987).
[18] W. M. Kosman and J. Hinze, J. Mol. Spectrosc. **56**, 93 (1975); C. R. Vidal and H. Scheingraber, *ibid.* **65**, 46 (1977).
[19] B. R. Johnson, J. Chem. Phys. **67**, 4086 (1977).
[20] L. F. Richardson, Philos. Trans. R. Soc. London, Ser. A **226**, 299 (1927).
[21] A. V. Abarenov and A. V. Stolyarov, J. Phys. B **23**, 2419 (1990).

[22] A. V. Stolyarov, N. E. Kuz'menko, Ya. A. Harya, and R. S. Ferber, J. Mol. Spectrosc. **137**, 251 (1989).
[23] P. A. Fraser, Can. J. Phys. **32**, 515 (1954).
[24] C. Noda and R. N. Zare, J. Mol. Spectrosc. **95**, 254 (1982); N. E. Kuz'menko and A. V. Stolyarov, J. Quant. Spectrosc. Radiat. Transf. **35**, 415 (1986).
[25] J. Tellinghuisen, Chem. Phys. Lett. **105**, 241 (1984).
[26] A. V. Stolyarov and V. I. Pupyshev, Phys. Rev. A **49**, 1693 (1994).
[27] E. A. Pazyuk, A. V. Stolyarov, and V. I. Pupyshev, Chem. Phys. Lett. **228**, 219 (1994).
[28] R. S. Ferber, Ya. A. Harya, and A. V. Stolyarov, J. Quant. Spectrosc. Radiat. Transf. **47**, 143 (1992).
[29] R. F. Barrow, R. M. Clements, J. Derouard, N. Sadeghi, C. Effantin, J. d'Incan, and A. J. Ross, Can. J. Phys. **65**, 1154 (1987).
[30] A. J. Ross, C. Effantin, J. d'Incan, and R. F. Barrow, Mol. Phys. **56**, 903 (1985).
[31] L. Lawson and R. J. Hanson, *Solving Least Squares Problems* (Prentice-Hall, Englewood Cliffs, NJ, 1974).
[32] P. Kowalczyk, J. Mol. Spectrosc. **136**, 1 (1989).
[33] A. J. Ross, R. M. Clements, and R. F. Barrow, J. Mol. Spectrosc. **127**, 546 (1988).
[34] W. L. Wiese, M. W. Smith, and B. M. Miles, *Atomic Transition Probabilities*, Natl.Stand.Ref.Data Soc., NBS Circ. No. 22 (USGPO, Washington, D.C. 1969), Vol. 2.
[35] J. A. Pople, J. W. McIver, and N. S. Ostlund, J. Chem. Phys. **49**, 2965 (1968).
[36] A. J. Sadlej, J. Chem. Phys. **75**, 320 (1981); G. H. F. Diercksen and A. J. Sadlej, *ibid.* **75**, 1253 (1981), and references therein.
[37] P. M. Kozlowski and E. R. Davidson, Int. J. Quantum Chem. **53**, 149 (1995).
[38] S. O. Adamson, A. Zaitsevskii and N. F. Stepanov (unpublished).
[39] R. Cimiraglia and A. Zaitsevskii (unpublished).
[40] K. Andersson, M. R. A. Blomberg, M. P. Fülscher, G. Karlström, V. Kellö, R. Lindh, P.-A. Malmqvist, J. Noga, J. Olsen, B. O. Roos, A. J. Sadlej, P. E. M. Siegbahn, M. Urban, P.-O. Wildmark. MOLCAS-3, University of Lund, Sweden, 1995.
[41] A. J. Sadlej and M. Urban, J. Mol. Struct.: THEOCHEM **234**, 147 (1991).
[42] A. Zaitsevskii and J. P. Malrieu, Chem. Phys. Lett. **250**, 366 (1996).
[43] J. P. Malrieu, J.-L. Heully, and A. Zaitsevskii, Theor. Chim. Acta **90**, 167 (1995).
[44] J. P. Malrieu, in *Recent Progress in Many-body Theories*, edited by E. Schachinger, H. Mitter, and H. Sormann (Plenum, New York, 1995), Vol. 4, p. 109.
[45] W. J. Stevens, D. D. Konowalow, and L. B. Ratcliff, J. Chem. Phys. **80**, 1215 (1984).
[46] K. P. Huber and G. Herzberg, *Molecular Spectra and Molecular Structure. IV. Constants of Diatomic Molecules* (van Nostrand, New York, 1979).
[47] P. J. Ellis and E. Osnes, Rev. Mod. Phys. **49**, 777 (1977).
[48] H. Sun and K. F. Freed, J. Chem. Phys. **88**, 2659 (1988); V. Hurtubise and K. F. Freed, Adv. Chem. Phys. **83**, 465 (1993).